Original Article

Dynamics and Morphology of Focal Adhesions in Complex 3D Environment

(focal adhesions, 3D, dermis-based matrix, adhesion, migration)

O. TOLDE[1,3], D. RÖSEL[1], R. JANOŠTIAK[1], P. VESELÝ[2], J. BRÁBEK[1]

[1]Department of Cell Biology, Faculty of Science, Charles University in Prague, Czech Republic
[2]CEITEC – Central European Institute of Technology, Brno University of Technology, Brno, Czech Republic
[3]Department of Molecular Medicine, Max Planck Institute of Biochemistry, Martinsried, Germany.

Abstract. Focal adhesions are specific types of cellular adhesion structures through which both mechanical force and regulatory signals are transmitted. Recently, the existence of focal adhesions in 3D environment has been questioned. Using a unique life-like model of dermis-based matrix we analysed the presence of focal adhesions in a complex 3D environment. Although the dermis-based matrix constitutes a 3D environment, the interface of cell-to-matrix contacts on thick bundled fibres within this matrix resembles 2D conditions. We call this a quasi-2D situation. We suggest that the quasi-2D interface of cell-to-matrix contacts constituted in the dermis-based matrix is much closer to _in tissue_ conditions than the meshed structure of mostly uniform thin fibres in the gel-based matrices. In agreement with our assumption, we found that the cell adhesion structures are formed by cells that invade the dermis-based matrix and that these structures are of similar size as focal adhesions formed on fibronectin-coated coverslips (2D). In both 2D situation and the dermis-based matrix, we observed comparable vinculin dynamics in focal adhesions and comparable enlargement of the focal adhesions in response to a MEK inhibitor. We conclude that focal adhesions that are formed in the 3D environment are similar in size and dynamics as those seen in the 2D setting.

Introduction

Focal adhesions (FAs) were first described in 1971 as regions in the fibroblast that had closer contact to the substratum than the other regions of cell surface (Abercrombie et al., 1971). Today, FAs are defined as specific types of cellular adhesion structures through which both mechanical force and regulatory signals are transmitted (Chen et al., 2003). The molecular composition, dynamics and signalling downstream of FAs have been reviewed recently (Geiger et al., 2001; Block et al., 2008; Geiger et al., 2009; Legate et al., 2009; Parsons et al., 2010).

FAs are typically observed and studied in cells grown in 2D systems, e.g. tissue culture dishes or coverslips. It is only in the last decade that FAs have been studied in a 3D environment (for review see Harunaga and Yamada, 2011). Cukierman et al. (2001) have shown that fibroblasts in cell-derived matrix have distinct cell-matrix adhesions that contain both integrins and vinculin. Tamariz and Grinnell (2002) directly compared fibroblasts embedded in collagen gels of two different densities and observed that cells in higher-density collagen gels have more protrusions with discrete cell matrix adhesions containing vinculin. Adhesion structures in cells embedded in 3D collagen were also documented in vascular smooth muscle cells (Li et al., 2003) and breast carcinoma cells (Wozniak et al., 2003). Studies of endothelial cells and fibroblasts in different types of 3D matrix – collagen, laminin, fibrin and cell-derived matrix – have described cell adhesions within 3D matrices in terms of quantity and size (Zhou et al., 2008; Hakkinen et al., 2011).

Live cell imaging is essential to prove that cell adhesion structures observed are not artifacts. The first demonstration that zyxin-containing cell adhesions exist in living fibroblasts within a 3D collagen gel was provided by Petroll et al. (2003). More recently, however, the existence of FAs in 3D environment has been questioned (Fraley et al., 2010). The authors showed that the formation and size of FAs in living sarcoma cells is distributed according to the topology of the cell inside the gel but

found to be missing in 3D conditions. However, Kubow and Horwitz (2011) revealed FAs in living sarcoma cells by reducing the background fluorescence. Further evidence for the presence of 3D cell adhesions in living cells was provided by Deakin and Turner (2011), who showed that GFP-talin could identify discrete adhesions in breast carcinoma cells in a 3D cell-derived matrix. The existence and interaction between FAs and the extracellular matrix is crucial to the understanding of malignant cell behaviour.

Therefore, in order to address the question of FA existence in 3D, we studied FAs within a life-like substrate of acellular porcine dermis. This substrate was successfully used by us previously to elucidate the structure of invadopodia in a complex 3D environment (Tolde et al., 2010). The dermis-based matrix exhibits minimal tensile strength of 4 MPa in the wet condition (data from manufacturer), which indicates collagen fibres much stiffer than would be required for formation of cell adhesions in 2D (Balaban et al., 2001). Using this life-like 3D matrix with remnants of basal membrane and apparently still containing growth factors (Hoganson et al., 2010), we avoided a deficit in natural toughness of reconstituted collagen fibres, lack of glycosaminoglycans as well as of growth factors embedded in the extracellular matrix (ECM). The dermis-based matrix, unlike fragile artificial gels, is a dense material which can sustain harsh washing conditions. Accordingly, problems with background fluorescence are minimized.

Material and Methods

Cell culture

RsK4 sarcoma cells were cultivated in full DMEM medium: DMEM (GIBCO, Grand Island, NY) with 4500 mg/l L-glucose, L-glutamine, and pyruvate, supplemented with 10% foetal bovine serum (Sigma-Aldrich, St. Louis, MO), 2% antibiotic-antimycotic (GIBCO) and 1% MEM non-essential amino acids (GIBCO). Dermis-based matrix: pig dermal cell-free matrix (XeDerma®; registered trade mark of BIO-SKIN a. s., Prague, Czech Republic) is a sterile wound covering biocompatible material made of porcine skin grafts prepared by removing the epidermis and all other cells. The matrix is stored in form of dry sheets. For immunofluorescence staining: two days before use the dermis was cut into small pieces (approximately 1 cm×1 cm), placed into 12-well plates with HBSS buffer and just prior to use washed twice with DMEM medium, and cells were seeded on the dermis and allowed to invade for two days. After incubation the dermis was washed with PBS and fixed. For labelling the dermis was pre-incubated for two days in HBSS buffer. The conjugation of FITC (1 μg/ml; Molecular Probes, Grand Island, NY) or Alexa Fluor 633 (0.5 μg/ml; Molecular Probes) was performed in 0.1M sodium bicarbonate buffer, pH 9.0 for 30 min and then the unconjugated dye was washed three times with PBS and two times with DMEM. RsK4 sarcoma cells were developed by the authors of this study and thus guaranteed to be of correct lineage.

Scanning electron microscopy (SEM)

RsK4 cells were seeded on dermis-based matrix and allowed to invade for two days. The dermis-based matrix with invading cells was washed two times in PBS, fixed in 2.5% glutaraldehyde, and washed again three times. Dehydration in increasing concentrations of ethanol (10 min each for 30%, 50%, 70%, 80%, 90%, 95% and 100%) was followed by critical point drying using CPD 030 (BAL TEC) coated with 3 nm gold in Bal-Tec Sputter Coater SCD 050 (Capovani Brothers Inc., Scotia, NY) and visualization in JEOL JSM-6380 LV (JEOL, Tokyo, Japan). Images were coloured using Adobe Photoshop.

Immunofluorescence microscopy

Invading RsK4 cells in the dermis-based matrix were fixed in 4% paraformaldehyde, permeabilized in 0.5% Triton X-100, washed thrice with PBS, and then blocked in 3% bovine serum albumin, incubated with primary antibody for 2 h, washed, incubated with secondary antibody for 60 min, then washed again, stained for 15 min with DY-405-phalloidin (Dyomics, Jena, Germany) or Alexa Fluor 488-phalloidin (Molecular Probes) and mounted. The primary antibodies were: anti phospho-paxillin (Tyr118; Cell Signaling Technology, Danvers, MA), anti phospho-FAK (Y397; Invitrogen, Carlsbad, CA), and anti-CAS clone 24 (BD Biosciences, San Jose, CA). The secondary antibodies were: anti-rabbit (Alexa Fluor 546, Molecular Probes) and anti-mouse (Alexa Fluor 633, Molecular Probes). Interference reflection images were visualized using the 488-nm line of an argon laser with AOBS setting of maximum detection of reflected light at 50 %. Images were acquired by the Leica TCS SP2 microscope system (Leica Mikrosysteme Vertrieb GmbH, Wetzlar, Germany) using Leica 63×/1.45 and 20×/0.7 oil objectives. Reflection images were processed for enhanced contrast to clearly visualize fibres using Adobe Photoshop. Merged images were prepared using ImageJ.

Fluorescence recovery after photobleaching (FRAP)

FRAP studies were conducted on live cells expressing YFP-tagged vinculin. The cells were plated on glass bottom dishes (MatTek) coated with 10 μg/ml fibronectin and cultured for 24 h before the experiment. For experiments in 3D, Alexa Fluor 633-stained pieces of dermis-based matrix were placed in MatTek dishes. Transfected cells were plated on the dermis two days prior to analysis. Only such FAs that were obviously formed on fibres were measured. Measurements were performed in DMEM, at 37 °C and 5 % CO_2. Focal adhesions, each structure from a different cell, expressing YFP-vinculin were analysed. After a brief measurement at monitoring intensity (488 nm), a high energy beam

was used to bleach 20–50 % of the fluorescence intensity in the area corresponding to the whole FA. The intensity of recovery of the bleached region was extracted from the image series and curves were fitted to single exponential functions. The characteristic fluorescence recovery time was extracted from the FRAP curves by nonlinear regression analysis, fitting to an exchange process.

Statistical analysis

Statistical significances were determined using ANOVA analysis in Statistica program (StatSoft, Tulsa, OK). Two-way ANOVA was performed to analyse the effect of MEK inhibitor and 2D vs. 3D conditions on FA length, one-way ANOVA was used to analyse statistical significance of the half-life recovery of vinculin between 2D and 3D. Nonlinear regression analysis of FRAP data was performed in DataFit (Oakdale Engineering, Oakdale, PA). The FRAP data were fit assuming one-phase exponential association from bottom to span plus bottom equation: Y (fluorescence recovery) = Span*(1-exp(-K*X))+bottom. The half-life time for recovery was calculated as 0.69/K.

Results

To analyse formation of FAs in the dermis-based matrix we have used the highly invasive RsK4 sarcoma cells. These cells invade the dermis-based matrix employing a mesenchymal mode that is dependent on proteolytic degradation of the matrix (Tolde et al., 2010). We have imaged invading RsK4 sarcoma cells in the dermis-based matrix. The collagen fibres were either labelled using FITC (Fig. 1A), or imaged in reflectance mode (Fig. 1B). The cells were mostly multi-polar with two or more protrusions of variable size and shape that extended out from the cell body, spanned multiple focal planes, and exhibited numerous adhesions. High-spatial-resolution imaging of the protrusions revealed that distinct adhesion structures of the cells are in contact to the adjacent fibres of the dermis-based matrix (Fig. 1A, B).

To confirm that the adhesion structures observed in invading cells represent FAs, we analysed the effect of MEK inhibitor U0126 on their length. The inhibition of MEK using U0126 increases the length of FAs (Vomastek et al., 2007), probably by reducing the rate of FA disassembly (Webb et al., 2004). When seeded on fibronectin-coated coverslips, the RsK4 cells formed typical FAs on the cell periphery marked by phospho-FAK and phospho-paxilin (Fig. 2A). In the central region the RsK4 cells developed podosomal structures (Fig. 2A), a characteristic of cells with high matrix degradation capacity.

First, we analysed the length of FAs formed in RsK4 cells plated on the 2D surface of fibronectin-coated cover glass. The average length of FAs was 850 nm (N = 55) and treatment with MEK inhibitor U0126 led to a significant increase of the average FA length to 1523 nm (N = 150) (Fig. 2). The adhesion structures of invading
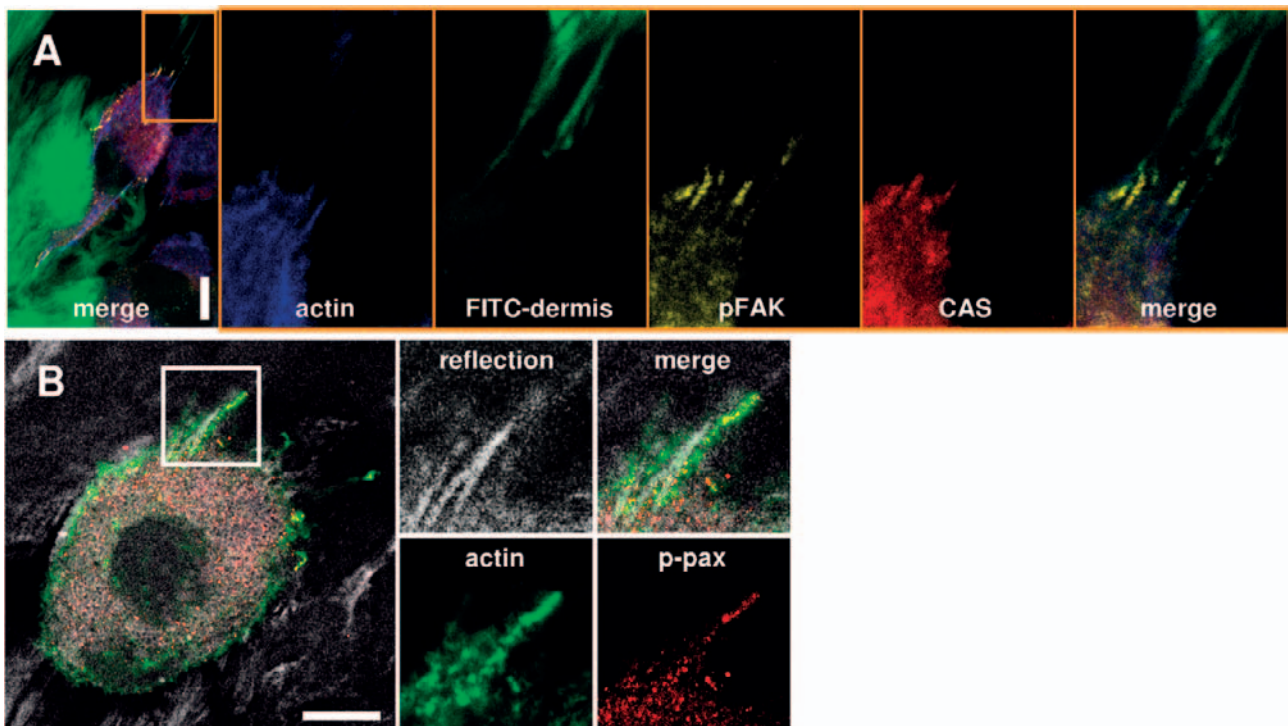

Fig. 1. Confocal microscopy imaging of adhesion structures in RsK4 cells invaded in dermis-based matrix. Adhesion structures are visualized as elongated structures at the distal edge of cellular protrusion in contact with fibres of dermis-based matrix. Adhesions are marked by co-localization of either (A) F-actin (blue) with phospho-FAK (yellow) and CAS (red) or (B) F-actin (green) with phospho-paxillin (red). The dermis-based matrix fibres are shown (A) FITC-labelled in green or (B) using confocal reflection in grey. The side panels show individual image channels and their merge of representative adhesive structures. Scale bars: 10 μm.
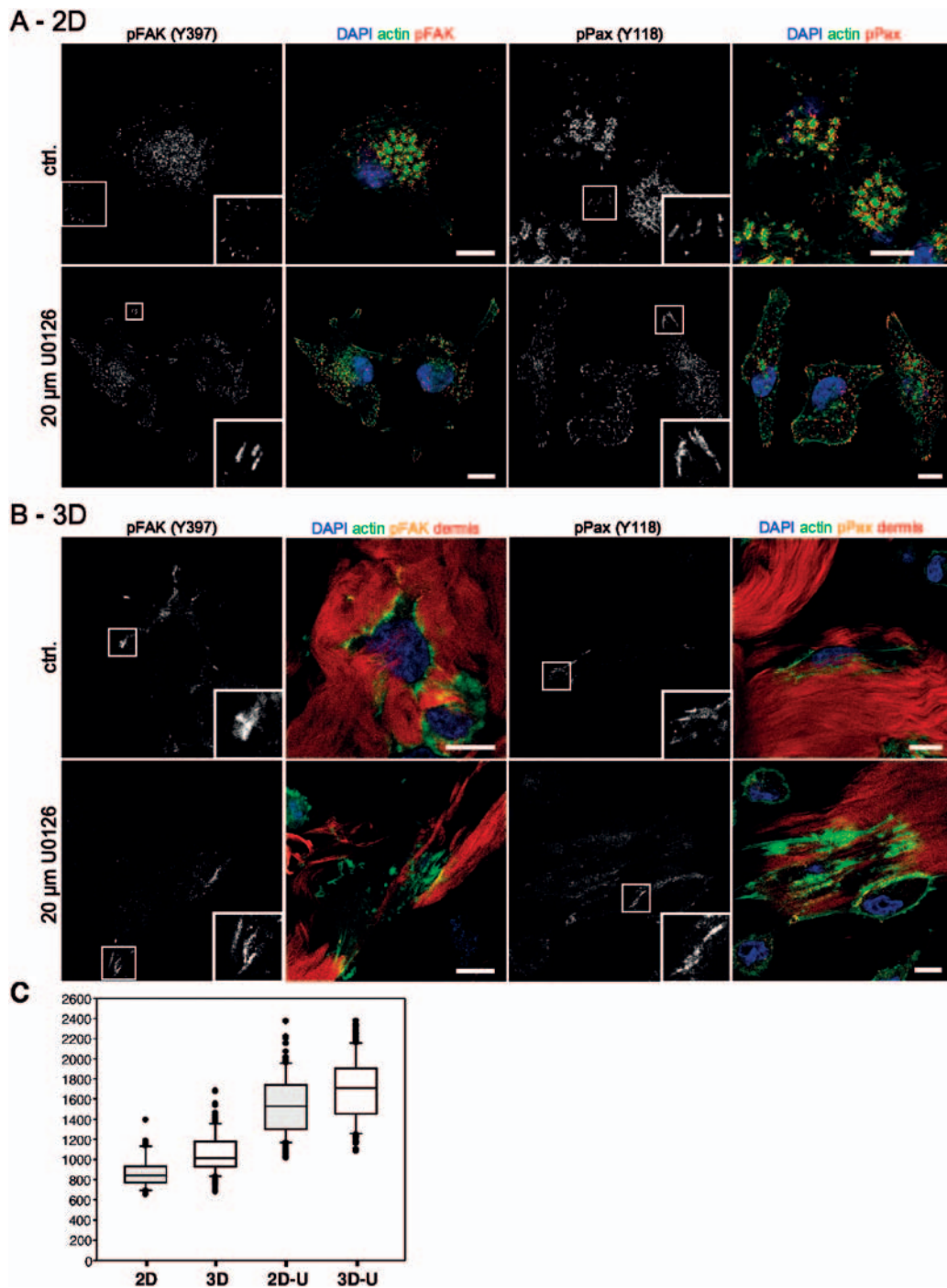
Fig. 2. The effect of MEK inhibitor U0126 on the size of adhesion structures in 2D and 3D environments. (A-2D) RsK4 cells were seeded on fibronectin-coated coverslips and stained for nuclei (blue), F-actin (green) and phospho-FAK (red, left) or phospho-paxillin (red, right) with or without (ctrl.) 20 μM U0126. Prominent adhesion structures marked by rectangles are shown in insets of red channel (grey). Note also the podosomes – rounded actin-rich structures in central region of the cells. (B-3D) RsK4 cells invaded in dermis-based matrix (red) were stained for nuclei (blue), F-actin (green) and phospho-FAK (orange, left) or phospho-paxillin (orange, right) with or without (ctrl.) 20 μM U0126. Prominent adhesion structures marked by rectangles are shown in insets of orange channel (grey). Scale bars: 10 μm. (C) Box and whisker plots for adhesion structure length of RsK4 cells grown in 2D or invaded in dermis-based matrix (3D) with or without 20 μM U0126 (U). The middle line of the box indicates median length, the top of the box indicates 75th percentile, the bottom of the box indicates 25th percentile, and the whiskers indicate the extent of 10th and 90th percentiles. Outside and far out values are displayed as separate points. Statistical analysis of the effect of 2D vs. 3D conditions and presence or absence of 20 μM U0126 on FA length was performed using a two-way ANOVA. The analysis revealed a statistically significant effect of 20 μM U0126 on FA length; addition of 20 μM U0126 led to development of longer FAs (ANOVA: $F_{(1,500)} = 589.61$, $P < 0.001$)). However, we found no effect of 2D vs. 3D conditions on FA length (ANOVA: $F_{(1,500)} = 0.40$, $P = 0.526$)). The interaction between factors was not significant (ANOVA: $F_{(1,500)} = 0.54$, $P = 0.464$)).
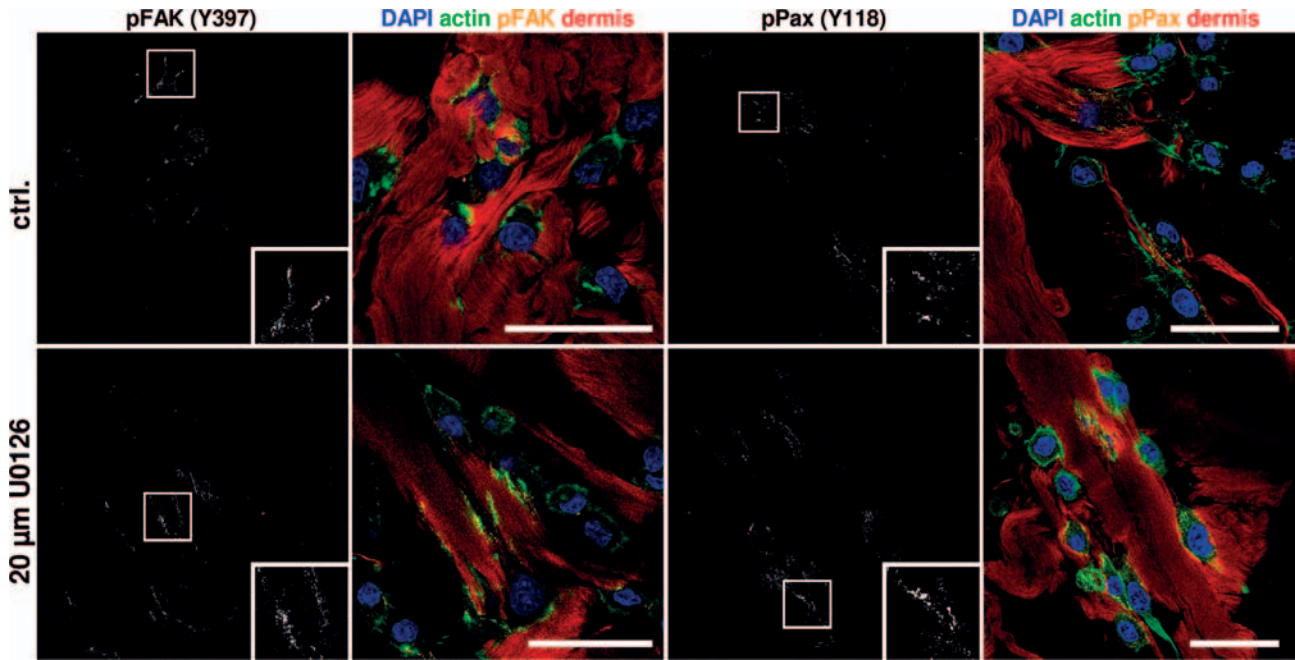
Fig. 3. Focal adhesions in dermis-based matrix are formed preferably on thick bundles of fibres. RsK4 cells invaded in dermis-based matrix (red) were stained for nuclei (blue), F-actin (green) and phospho-FAK (orange, left) or phospho-paxillin (orange, right) with or without (ctrl.) 20 μM U0126. Prominent adhesion structures marked by rectangles are shown in insets of orange channel (grey). Scale bars: 50 μm
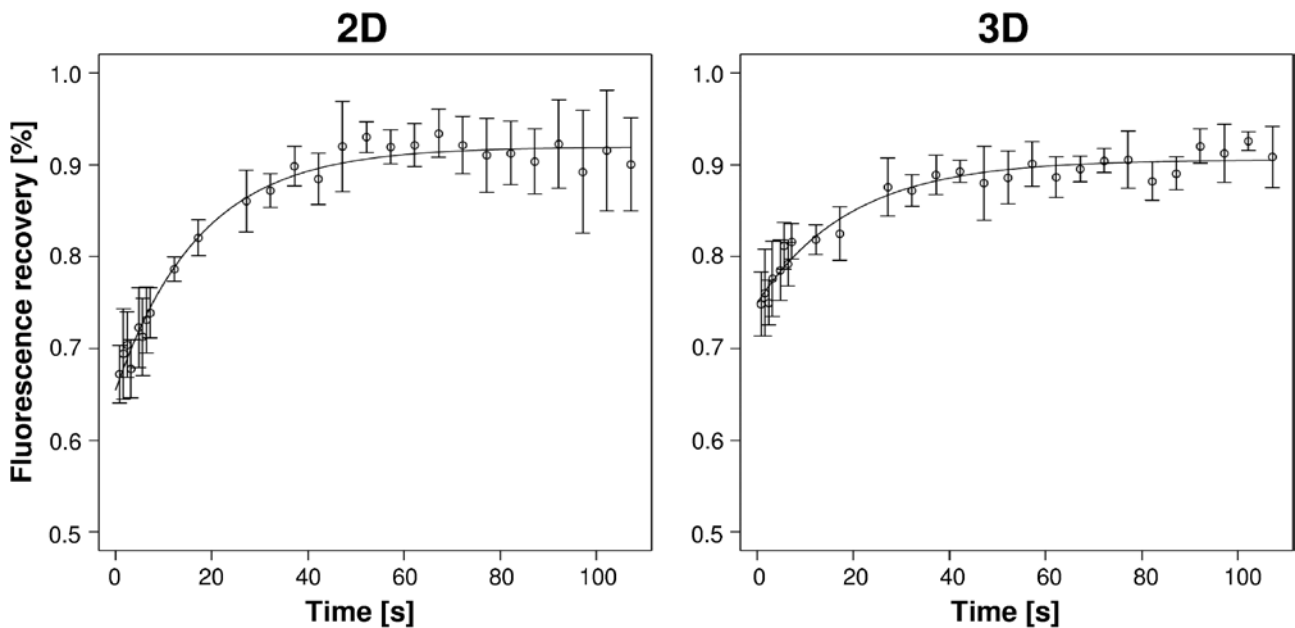

Fig. 4. FRAP analysis of FA dynamics in 2D and 3D environments. RsK4 cells transfected with YFP-vinculin were seeded on fibronectin-coated coverslips (left) or allowed to invade the dermis-based matrix (right) and subjected to FRAP analysis. The data are shown as mean recovery with error bars representing standard errors. FRAP curves were modelled assuming one-phase exponential association from bottom to span plus bottom equation. The coefficient of determination (R^2) for the fitted curves is 0.98 for the dynamics in 2D and 0.95 for the dynamics in 3D.

RsK4 cells were slightly longer (1075 nm, N = 156) but not significantly different from those in 2D (Fig. 3). The adhesion structures formed in invading RsK4 cells responded similarly to MEK inhibitor U0126. The length of the adhesion structures increased to 1690 nm (N = 150) (Fig. 2). Taken together, the adhesion structures observed in the invading RsK4 cells were similar in size

to those seen in the 2D environment and responded similarly to MEK inhibitor U0126 (Fig. 2). This suggests that adhesion structures observed in invading RsK4 cells are in fact FAs.

A closer examination of cells inside the dermis-based matrix revealed that FAs are formed preferably on thick bundles of fibres with cells oriented alongside these
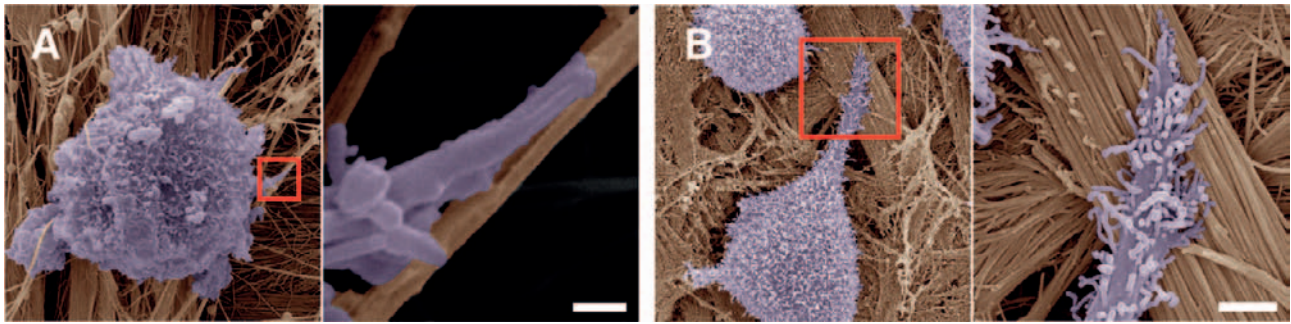
Fig. 5. Scanning electron microscopy of adhesion structures in RsK4 cells invaded in dermis-based matrix. RsK4 cells were seeded on dermis-based matrix and allowed to invade for two days. SEM images show RsK4 cells in shallow cavities within the dermis-based matrix. The invaded RsK4 cell is in contact with thin (ca 0.3 μm) (A) or thick (ca 6 μm) (B) aggregates of collagen fibres. Right panels: Details of a representative contact structure attached to collagen fibres (regions marked by rectangles on left panels). Scale bars: 0.5 μm (A), 2 μm (B).

thick bundles (Fig. 3). Taken together, these observations indicate that cells preferably invade/move alongside thick bundles inside the matrix.

To further analyse the FAs formed in the dermis-based matrix we examined the dynamic exchange of vinculin in FAs formed in 2D and 3D environments. The RsK4 cells were transiently transfected to express YFP-vinculin and the exchange rates of YFP-vinculin in FAs at the periphery of the cells were determined (Fig. 4). The FRAP experiments revealed that recovery half-life for vinculin is comparable in both 2D (12.0 ± 2.7 s) and 3D environments (13.4 ± 3.8 s; $P = 0.57$).

To visualize the contacts between cells and extracellular matrix in detail, the RsK4 cells seeded on dermis-based matrix were visualized by scanning electron microscopy (SEM). After invading the dermis-based matrix the RsK4 cells are mostly found on the bottom of cavities apparently made by their protease activity (Tolde et al., 2010). We observed lateral cellular protrusions with close contact to fibres of the matrix, suggesting formation of adhesion structures at the protrusion-to-fibre contact. Not surprisingly, we found that the size of contact structures was limited by the size of collagen fibres. Thin fibres (with average diameter 0.3 μm) were in contact with thin protrusions, suggesting small adhesion contacts (Fig. 5). On thick aggregates of fibres (diameter 3–8 μm), the protrusions were much larger and the size of contact structures suggestes that larger adhesions were probably composed of multiple individual adhesions (Fig. 5).

Discussion

Disagreements on the existence of FAs in 3D collagen gels (Fraley et al., 2010; Harunaga and Yamada, 2011; Kubow and Horwitz, 2011) prompted us to analyse the structure and dynamics of cell adhesion structures in a 3D environment using a life-like dermis-based matrix.

According to Fraley et al. (2011), FAs cannot be formed in a 3D environment. Their experiments analysing formation of FAs in 3D were performed on reconstituted collagen gels. Even though the fibrillar structure of these gels resembles the *in vivo* situation, it is still different from an *in tissue* environment. Although these gels simulate a 3D environment, it is an artificial system – homogenous environment, where fibres are thin and unbundled with cross-linking of the fibres dependent on the method of extraction (Sabeh et al., 2009). The collagen fibres in the ECM appear quasi-one-dimensional, which limits the size of FAs and the associated clusters of integrins (Wirtz et al., 2011). The diameter of the ECM fibres is typically in the order of 100 nm (Raub et al., 2007). FAs formed in 2D substrates are typically about 1 μm in size, which is approximately one order larger than the diameter of ECM fibres. Thus the larger adhesions may not be formed deep inside the gels composed of thin fibres only. In addition, the thin collagen fibres may not be stiff enough to withstand the tension necessary for FA formation (Ulrich et al., 2009; Brabek et al., 2010).

Intravital imaging shows that cancer cells and leukocytes migrate on thick collagen fibres (Wang et al., 2002; Condeelis and Segall, 2003; Wyckoff et al., 2007). These thick bundles may be of 10 μm or more in diameter. Cancer cells can use these thick fibres as migration highways (Egeblad et al., 2010). In the dermis-based matrix, the RsK4 cells were often observed to be associated with thick collagen bundles (i. e. seen in Fig 3, bottom right panel), suggesting that they employ a similar migratory and invasive strategy. Adhesion structures formed within these bundles have a morphology and dynamics that is similar to FAs formed in 2D. Although the dermis-based matrix constitutes a 3D environment, the interface of cell-to-matrix contacts on these bundled fibres resembles 2D conditions, rather than the meshed structure of mostly uniform thin fibres in artificial gels. We call this a quasi-2D situation. We suggest that the quasi-2D interface of cell-to-matrix contact constituted in the dermis-based matrix is much closer to *in tissue* conditions than the uniform structure of gel-based matrices.

It is important to note that the role of focal adhesion proteins in 2D cell motility might not be predictive of

their role in 3D matrices, and that the structure and dynamics of adhesions in gels might not be predictive of their role in tissues. Our study shows that the structure and dynamics of FAs is similar in 2D and on quasi-2D interfaces. The dermis-based matrix thus represents a promising tool for the analysis of adhesive structures and cell migration in the close to *in tissue* environment.

References

Abercrombie, M., Heaysman, J. E., Pegrum, S. M. (1971) The locomotion of fibroblasts in culture. IV. Electron microscopy of the leading lamella. *Exp. Cell Res.* **67**, 359-367.

Balaban, N. Q., Schwarz, U. S., Riveline, D., Goichberg, P., Tzur, G., Sabanay, I., Mahalu, D., Safran, S., Bershadsky, A., Addadi, L., Geiger, B. (2001) Force and focal adhesion assembly: a close relationship studied using elastic micropatterned substrates. *Nat. Cell Biol.* **3**, 466-472.

Block, M. R., Badowski, C., Millon-Fremillon, A., Bouvard, D., Bouin, A. P., Faurobert, E., Gerber-Scokaert, D., Planus, E., Albiges-Rizo, C. (2008) Podosome-type adhesions and focal adhesions, so alike yet so different. *Eur. J. Cell Biol.* **87**, 491-506.

Brabek, J., Mierke, C. T., Rosel, D., Vesely, P., Fabry, B. (2010) The role of the tissue microenvironment in the regulation of cancer cell motility and invasion. *Cell Commun. Signal.* **8**, 22.

Chen, C. S., Alonso, J. L., Ostuni, E., Whitesides, G. M., Ingber, D. E. (2003) Cell shape provides global control of focal adhesion assembly. *Biochem. Biophys. Res. Commun.* **307**, 355-361.

Condeelis, J., Segall, J. E. (2003) Intravital imaging of cell movement in tumours. *Nat. Rev. Cancer* **3**, 921-930.

Cukierman, E., Pankov, R., Stevens, D. R., Yamada, K. M. (2001) Taking cell-matrix adhesions to the third dimension. *Science* **294**, 1708-1712.

Deakin, N. O., Turner, C. E. (2011) Distinct roles for paxillin and Hic-5 in regulating breast cancer cell morphology, invasion, and metastasis. *Mol. Biol. Cell* **22**, 327-341.

Egeblad, M., Rasch, M. G., Weaver, V. M. (2010) Dynamic interplay between the collagen scaffold and tumor evolution. *Curr. Opin. Cell Biol.* **22**, 697-706.

Fraley, S. I., Feng, Y., Krishnamurthy, R., Kim, D. H., Celedon, A., Longmore, G. D., Wirtz, D. (2010) A distinctive role for focal adhesion proteins in three-dimensional cell motility. *Nat. Cell Biol.* **12**, 598-604.

Fraley, S. I., Feng, Y., Wirtz, D., Longmore, G. D. (2011) Reply: reducing background fluorescence reveals adhesions in 3D matrices. *Nat. Cell Biol.* **13**, 5-7.

Geiger, B., Bershadsky, A., Pankov, R., Yamada, K. M. (2001) Transmembrane crosstalk between the extracellular matrix-cytoskeleton crosstalk. *Nat. Rev. Mol. Cell Biol.* **2**, 793-805.

Geiger, B., Spatz, J. P., Bershadsky, A. D. (2009) Environmental sensing through focal adhesions. *Nat. Rev. Mol. Cell Biol.* **10**, 21-33.

Hakkinen, K. M., Harunaga, J. S., Doyle, A. D., Yamada, K. M. (2011) Direct comparisons of the morphology, migration, cell adhesions, and actin cytoskeleton of fibroblasts in four different three-dimensional extracellular matrices. *Tissue Eng. Part A* **17**, 713-724.

Harunaga, J. S., Yamada, K. M. (2011) Cell-matrix adhesions in 3D. *Matrix Biol.* **30**, 363-368.

Hoganson, D. M., O'Doherty, E. M., Owens, G. E., Harilal, D. O., Goldman, S. M., Bowley, C. M., Neville, C. M., Kronengold, R. T., Vacanti, J. P. (2010) The retention of extracellular matrix proteins and angiogenic and mitogenic cytokines in a decellularized porcine dermis. *Biomaterials* **31**, 6730-6737.

Kubow, K. E., Horwitz, A. R. (2011) Reducing background fluorescence reveals adhesions in 3D matrices. *Nat. Cell Biol.*, **13**, 3-5.

Legate, K. R., Wickstrom, S. A., Fassler, R. (2009) Genetic and cell biological analysis of integrin outside-in signaling. *Genes Dev.* **23**, 397-418.

Li, S., Lao, J., Chen, B. P., Li, Y. S., Zhao, Y., Chu, J., Chen, K. D., Tsou, T. C., Peck, K., Chien, S. (2003) Genomic analysis of smooth muscle cells in 3-dimensional collagen matrix. *FASEB J.* **17**, 97-99.

Parsons, J. T., Horwitz, A. R., Schwartz, M. A. (2010) Cell adhesion: integrating cytoskeletal dynamics and cellular tension. *Nat. Rev. Mol. Cell Biol.* **11**, 633-643.

Petroll, W. M., Ma, L., Jester, J. V. (2003) Direct correlation of collagen matrix deformation with focal adhesion dynamics in living corneal fibroblasts. *J. Cell Sci.* **116**, 1481-1491.

Raub, C. B., Suresh, V., Krasieva, T., Lyubovitsky, J., Mih, J. D., Putnam, A. J., Tromberg, B. J., George, S. C. (2007) Noninvasive assessment of collagen gel microstructure and mechanics using multiphoton microscopy. *Biophys. J.* **92**, 2212-2222.

Sabeh, F., Shimizu-Hirota, R., Weiss, S. J. (2009) Protease-dependent versus -independent cancer cell invasion programs: three-dimensional amoeboid movement revisited. *J. Cell Biol.* **185**, 11-19.

Tamariz, E., Grinnell, F. (2002) Modulation of fibroblast morphology and adhesion during collagen matrix remodeling. *Mol. Biol. Cell* **13**, 3915-3929.

Tolde, O., Rosel, D., Vesely, P., Folk, P., Brabek, J. (2010) The structure of invadopodia in a complex 3D environment. *Eur. J. Cell Biol.* **89**, 674-680.

Ulrich, T. A., Juan Pardo, E. M., Kumar, S. (2009) The mechanical rigidity of the extracellular matrix regulates the structure, motility, and proliferation of glioma cells. *Cancer Res.* **69**, 4167-4174.

Vomastek, T., Iwanicki, M. P., Schaeffer, H. J., Tarcsafalvi, A., Parsons, J. T., Weber, M. J. (2007) RACK1 targets the extracellular signal-regulated kinase/mitogen-activated protein kinase pathway to link integrin engagement with focal adhesion disassembly and cell motility. *Mol. Cell Biol.* **27**, 8296-8305.

Wang, W., Wyckoff, J. B., Frohlich, V. C., Oleynikov, Y., Huttelmaier, S., Zavadil, J., Cermak, L., Bottinger, E. P., Singer, R. H., White, J. G., Segall, J. E., Condeelis, J. S. (2002) Single cell behavior in metastatic primary mammary tumors correlated with gene expression patterns revealed by molecular profiling. *Cancer Res.* **62**, 6278-6288.

Webb, D. J., Donais, K., Whitmore, L. A., Thomas, S. M., Turner, C. E., Parsons, J. T., Horwitz, A. F. (2004) FAK-Src signalling through paxillin, ERK and MLCK regulates adhesion disassembly. *Nat. Cell Biol.* **6**, 154-161.

Wirtz, D., Konstantopoulos, K., Searson, P. C. (2011) The physics of cancer: the role of physical interactions and mechanical forces in metastasis. *Nat. Rev. Cancer* **11**, 512-522.

Wozniak, M. A., Desai, R., Solski, P. A., Der, C. J., Keely, P. J. (2003) ROCK-generated contractility regulates breast epithelial cell differentiation in response to the physical properties of a three-dimensional collagen matrix. *J. Cell Biol.* **163**, 583-595.

Wyckoff, J. B., Wang, Y., Lin, E. Y., Li, J. F., Goswami, S., Stanley, E. R., Segall, J. E., Pollard, J. W., Condeelis, J. (2007) Direct visualization of macrophage-assisted tumor cell intravasation in mammary tumors. *Cancer Res.* **67**, 2649-2656.

Zhou, X., Rowe, R. G., Hiraoka, N., George, J. P., Wirtz, D., Mosher, D. F., Virtanen, I., Chernousov, M. A., Weiss, S. J. (2008). Fibronectin fibrillogenesis regulates three-dimensional neovessel formation. *Genes Dev.* **22**, 1231-1243.